ELSEVIER

Journal of Alloys and Compounds 426 (2006) 327–334

Journal of ALLOYS AND COMPOUNDS

www.elsevier.com/locate/jallcom

Influence of Mn-dopant on the properties of α-FeOOH particles precipitated in highly alkaline media

Stjepko Krehula, Svetozar Musić *

Division of Materials Chemistry, Ruđer Bošković Institute, P.O. Box 180, HR-10002 Zagreb, Croatia

Received 3 January 2006; received in revised form 3 February 2006; accepted 4 February 2006
Available online 29 March 2006

Abstract

The effects of Mn-dopant on the formation of solid solutions α-(Fe, Mn)OOH in dependence on the initial concentration ratio $r = [Mn]/([Mn] + [Fe])$, as well as on the size and morphology of the corresponding particles were investigated using Mössbauer and FT-IR spectroscopies, high-resolution scanning electron microscopy (FE SEM) and an energy dispersive X-ray analyser (EDS). The value of the hyperfine magnetic field of 34.9 T, as recorded for the reference α-FeOOH sample at RT, decreased linearly up to 21.4 T for sample with $r = 0.1667$. Only a paramagnetic doublet at RT was recorded for sample with $r = 0.2308$, a ferrite phase was additionally found for $r = 0.3333$. Fe–OH bending IR bands, δ_{OH} and γ_{OH}, were influenced by the Mn-substitution as manifested through their gradual shifts. FE SEM micrographs showed a great elongation of the starting acicular particles along the *c*-axis with an increase in Mn-doping. For $r = 0.1667$ and 0.2308 star-shaped and dendritic twin α-(Fe, Mn)OOH particles were observed. The length of these α-(Fe, Mn)OOH particles decreased, whereas their width increased. The α-Fe_2O_3 phase was not detected in any of the samples prepared.

Keywords: Mn-dopant; Tetramethylammonium hydroxide; α-FeOOH; ^{57}Fe Mössbauer; FT-IR; FE SEM

1. Introduction

Iron-oxyhydroxides and -oxides (group name: *iron oxides*) are widely spread in nature, for example in soils, sediments, rocks, lakes and seas. As a rule, they may contain different amounts of metal cations incorporated into their crystal structure. Synthetic *iron oxides* play an important role in various applications. They are used as pigments, catalysts, magnetic recording media, sensors, etc. The properties of synthetic *iron oxides* can be significantly changed upon incorporation of metal cations into their crystal structure. Over the past years researchers investigated the properties of doped *iron oxides* from an academic standpoint, as well as because of their role in natural processes and importance in industrial applications. In these investigations much attention was focused on doped α-FeOOH (goethite).

Berry et al. [1] investigated Sn-doped α-FeOOH and found that the ^{119}Sn Mössbauer spectra are consistent with the octahedral position of Sn^{4+} inside the α-FeOOH structure. It was suggested that the charge balance in Sn-doped α-FeOOH was achieved by the formation of cation vacancies.

Incorporation of trivalent cations into α-FeOOH has also been the subject of many investigations, the majority of which was linked with Al-doped α-FeOOH, because it occurs in nearly all soils and influences changes in the soil colour, size and morphology of soil particles, as well as changes in the adsorption capacity and a possible phase transformations. Lewis and Schwertmann [2] have found a linear correlation between the degree of Al^{3+} substitution and $\log [Al^{3+}]$ in aqueous solution for Al^{3+} incorporation up to 12 mol%. Fey and Dixon [3] showed that poorly crystalline and hydrated Al-doped α-FeOOH incorporated up to 30 mol% Al with a minimal deviation from Vegard's law. Murad and Schwertmann [4] investigated the influence of Al-substitution and crystallinity on the Mössbauer spectrum of α-FeOOH. Schulze [5] measured unit-cell dimensions of Al-substituted α-FeOOH and found that the *c* dimension was a linear function of Al-substitution up to 33 mol% Al, the *a* dimension was variable over the same concentration range, whereas the *b* dimension slightly deviated from linearity between 20 and 33 mol% Al. Cr-substituted α-FeOOH has also been investigated

* Corresponding author.
E-mail address: music@irb.hr (S. Musić).

0925-8388/$ – see front matter © 2006 Elsevier B.V. All rights reserved.
doi:10.1016/j.jallcom.2006.02.009

Table 1
Experimental conditions for the synthesis of samples G to MG11

Sample	2 M $FeCl_3$ (ml)	[$FeCl_3$] (M)	0.1 M $MnSO_4$ (ml)	0.01 M $MnSO_4$ (ml)	[$MnSO_4$] (M)	r = [Mn]/([Mn] + [Fe])	H_2O (ml)	TMAH (ml)
G	2	0.1	–	–	0	0	28	10
MG1	2	0.1	–	4	0.001	0.0099	24	10
MG2	2	0.1	–	8	0.002	0.0196	20	10
MG3	2	0.1	–	12	0.003	0.0291	16	10
MG4	2	0.1	2	–	0.005	0.0476	26	10
MG5	2	0.1	3	–	0.0075	0.0698	25	10
MG6	2	0.1	4	–	0.010	0.0909	24	10
MG7	2	0.1	5	–	0.0125	0.1111	23	10
MG8	2	0.1	6	–	0.015	0.1304	22	10
MG9	2	0.1	8	–	0.020	0.1667	20	10
MG10	2	0.1	12	–	0.030	0.2308	16	10
MG11	2	0.1	20	–	0.050	0.3333	8	10

[6,7], and these investigations are important for a better understanding of the role of α-(Fe, Cr)OOH as protective rust on the surface of weathering steel [8,9]. Dos Santos et al. [10] investigated the incorporation of Ga^{3+} ions into the α-FeOOH structure.

Incorporation of divalent metal cations into the α-FeOOH structure has also been the subject of investigations. Sileo et al. [11] found that for a final molar ratio $\mu_{Cd} \leq 5.50$ [expressed as $\mu_{Cd} = 100{\cdot}[Cd]/([Cd] + [Fe])$] only one solid solution α-(Fe, Cd)OOH was obtained. At $\mu_{Cd} = 7.03$ the incorporation of Cd^{2+} ions into the α-FeOOH structure was drastically reduced and Cd-substituted α-Fe_2O_3 was additionally obtained. Ni-substituted goethites from Vermelho deposits (Brazilian Amazonia [12] and synthetic α-FeOOH doped with Ni^{2+} ions [13,14] were also investigated. Stiers and Schwertmann [15] found by XRD about 15 mol% Mn incorporated into the α-FeOOH structure. The authors suggested that Mn^{2+} was oxidised to Mn^{3+}. Vandenberghe et al. [16] prepared Mn-substituted α-FeOOH, whereas Mn-substituted α-Fe_2O_3 was produced by heating as prepared α-(Fe, Mn)OOH at 500 °C. Incorporation of manganese ions into α-FeOOH caused a decrease in the hyperfine magnetic field which was smaller than in the case of Al^{3+} ions. On the other hand, a stronger influence on the Morin transition in α-$(Fe_{1-c}Mn_c)_2O_3$ was observed, giving rise to a weak ferromagnetic state at 80 K for $c > 0.04$. Cornell [17] investigated a simultaneous incorporation of Mn, Ni and Co into the α-FeOOH structure, and found that 2–4 mol% of each of the three cations were dissolved in the α-FeOOH structure. When two of these metal cations were simultaneously dissolved in the α-FeOOH,

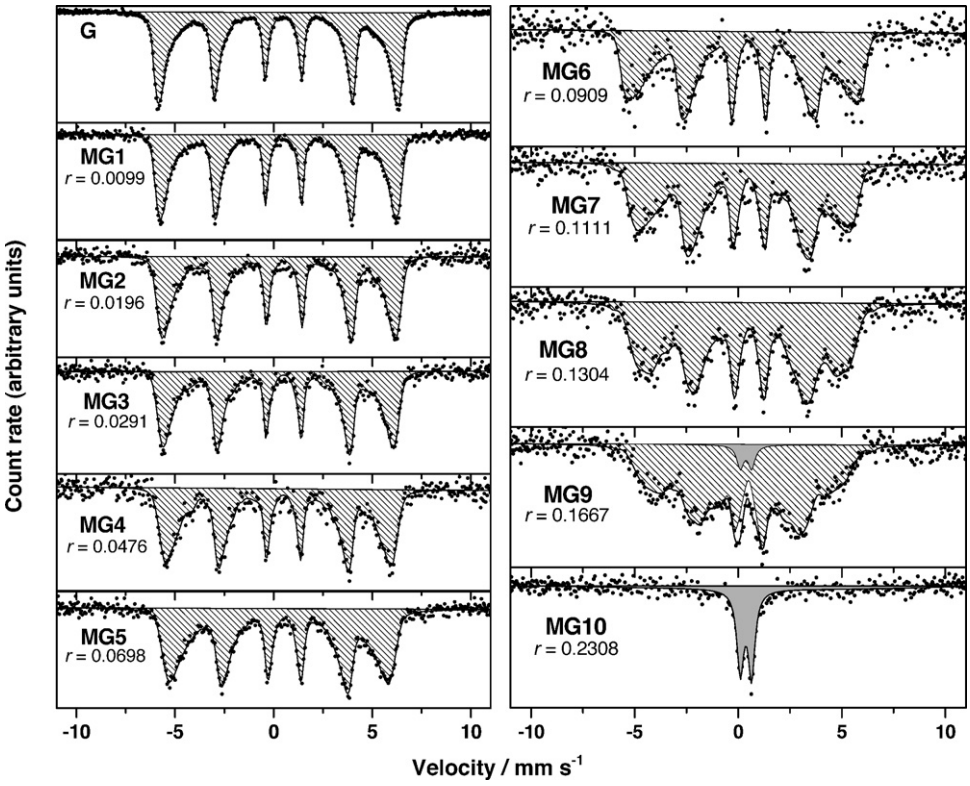

Fig. 1. ^{57}Fe Mössbauer spectra of samples G, MG1–MG10 recorded at RT.

Table 2
^{57}Fe Mössbauer parameters calculated for samples G to MG11 and identification

Sample	Spectral line	δ (mm s^{-1})	E_q or Δ (mm s^{-1})	B_{hf} (T)	Γ (mm s^{-1})	Area (%)	Identification
G	M	0.37	−0.26	34.9	0.26	100	α-FeOOH
MG1	M	0.37	−0.26	34.3	0.23	100	α-(Fe, Mn)OOH
MG2	M	0.37	−0.27	33.6	0.25	100	α-(Fe, Mn)OOH
MG3	M	0.37	−0.26	32.5	0.24	100	α-(Fe, Mn)OOH
MG4	M	0.37	−0.29	31.9	0.26	100	α-(Fe, Mn)OOH
MG5	M	0.38	−0.28	30.9	0.30	100	α-(Fe, Mn)OOH
MG6	M	0.37	−0.28	29.4	0.23	100	α-(Fe, Mn)OOH
MG7	M	0.38	−0.29	26.9	0.28	100	α-(Fe, Mn)OOH
MG8	M	0.39	−0.29	25.8	0.35	100	α-(Fe, Mn)OOH
MG9	M	0.39	−0.26	21.4	0.32	96.1	α-(Fe, Mn)OOH
	Q	0.37	0.55		0.39	3.9	
MG10	Q	0.37	0.55		0.39	100	α-(Fe, Mn)OOH
MG11	Q	0.37	0.64	–	0.39	40.3	α-(Fe, Mn)OOH
	M_1	0.37	−0.26	19.8	0.64	25.4	
	M_2	0.36	−0.14	50.4	0.39	9.7	
	M_3	0.34	0.03	48.1	0.49	13.4	$Mn_xFe_{3-x}O_4$
	M_4	0.34	−0.09	45.0	0.83	11.2	

Errors: $\delta = \pm 0.01$ mm s^{-1}, $E_q = \pm 0.01$ mm s^{-1}, $B_{hf} = \pm 0.2$ T. Isomer shift is given relative to α-Fe.

their fractions increased up to 6 mol% each. Singh et al. [18] monitored the incorporation of Cr^{3+}, Mn^{2+} and Ni^{2+} into α-FeOOH using the X-ray absorption fine structure (EXAFS) spectroscopy, whereas Morales et al. [19] investigated the properties of α-FeOOH crystallites grown in the presence of Cr^{3+}, Cu^{2+} and Mn^{2+} ions, using Mössbauer spectroscopy. Kusuyama et al. [20] investigated the influence of Mn-substitution in α-FeOOH on the adsorption capacities for Pb^{2+}, Cu^{2+} and Zn^{2+} ions.

The present work is focused on the effect of Mn-dopant on the precipitation of α-FeOOH in a highly alkaline pH. The precipitation of α-FeOOH was based on a novel synthesis route reported by Krehula et al. [21]. The aim of the present work was to: (a) investigate the incorporation of Mn-dopant into the α-FeOOH structure as a function of the initial concentration ratio $r = [Mn]/([Mn] + [Fe])$ and (b) investigate changes in the size and morphology of Mn-substituted α-FeOOH particles. This was possible due to the application of Mössbauer and FT-IR spectroscopies and a high-resolution scanning electron microscopy. ^{57}Fe Mössbauer spectroscopy is a particularly useful technique in the investigation of iron-containing materials [22].

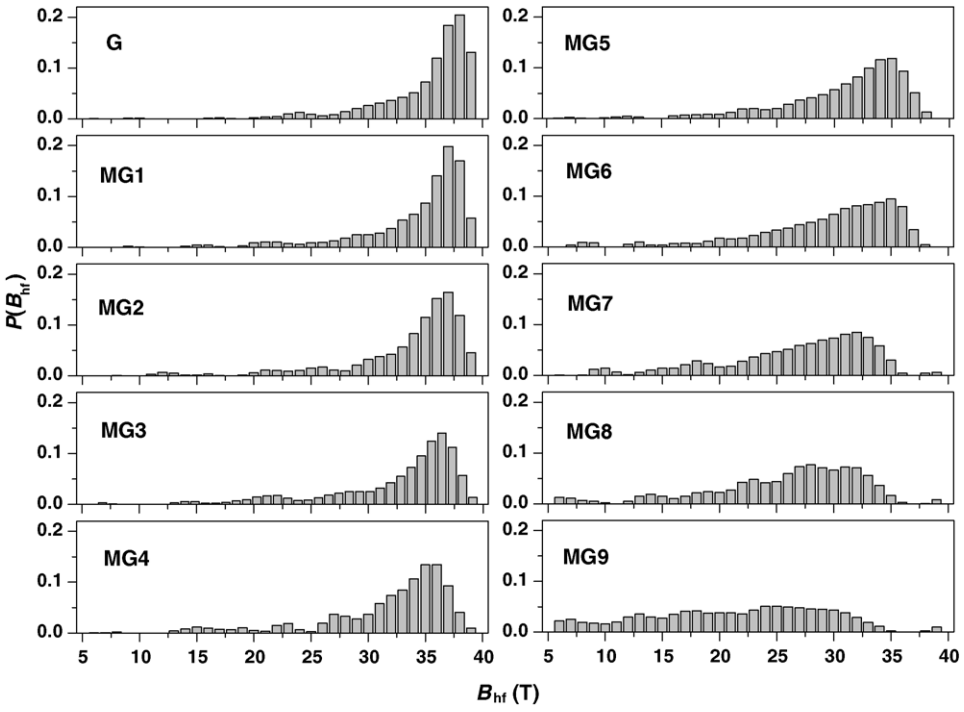

Fig. 2. Distributions of the hyperfine magnetic field calculated for reference α-FeOOH (sample G) and samples MG1–MG9.

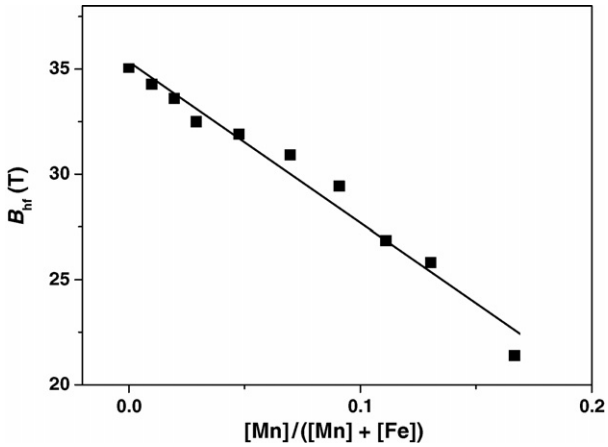

Fig. 3. Dependence of the average hyperfine magnetic field in α-FeOOH on the [Mn]/([Mn] + [Fe]) ratio.

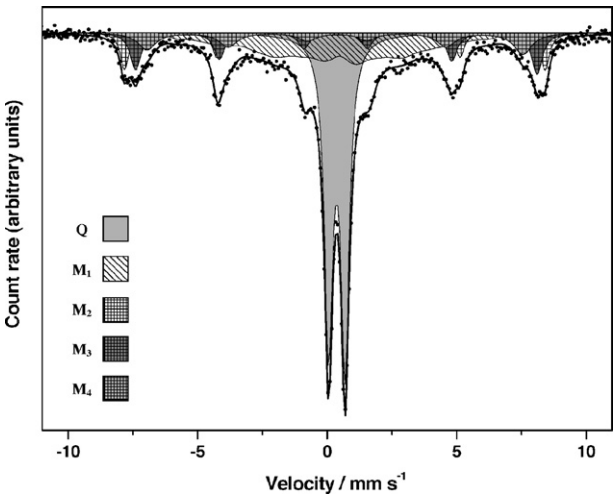

Fig. 4. ^{57}Fe Mössbauer spectrum of sample MG11 recorded at RT.

2. Experimental

2.1. Preparation of samples

The chemicals of analytical purity, $FeCl_3 \cdot 6H_2O$ and $MnSO_4 \cdot H_2O$ were supplied by Kemika. A tetramethylammonium hydroxide (TMAH) solution (25%, w/w, electronic grade 99.9999%) supplied by Alfa Aesar® was used. Twice-distilled water prepared in our own laboratory was used in all experiments. Predetermined volumes of $FeCl_3$ and $MnSO_4$ solutions and twice-distilled water were mixed, then TMAH was added as a precipitating agent. The exact experimental conditions for the preparation of samples are given in Table 1. The formed suspensions were vigorously shaken for ∼10 min, then heated at 160 °C, using the Parr general-purpose bomb (model 4744), comprising a Teflon vessel and cup. After 2 h of heating the precipitates were cooled to RT (mother liquor pH ∼13.5–13.8) and subsequently washed with twice-distilled water using the ultraspeed Sorvall RC2-B centrifuge. After drying, all precipitates were characterised by Mössbauer and FT-IR spectroscopies, as well as high-resolution scanning electron microscopy. The results of EDS analyses of the precipitates were consistent with the nominal concentrations of iron and manganese.

2.2. Instrumentation

^{57}Fe Mössbauer spectra were recorded in transmission mode using a standard WISSEL GmbH (Starnberg, Germany) instrumental configuration. ^{57}Co in rhodium matrix was used as a Mössbauer source. The velocity scale and all the data refer to metallic α-Fe absorber at RT. A quantitative analysis of the recorded spectra was made using the MOSSWINN program.

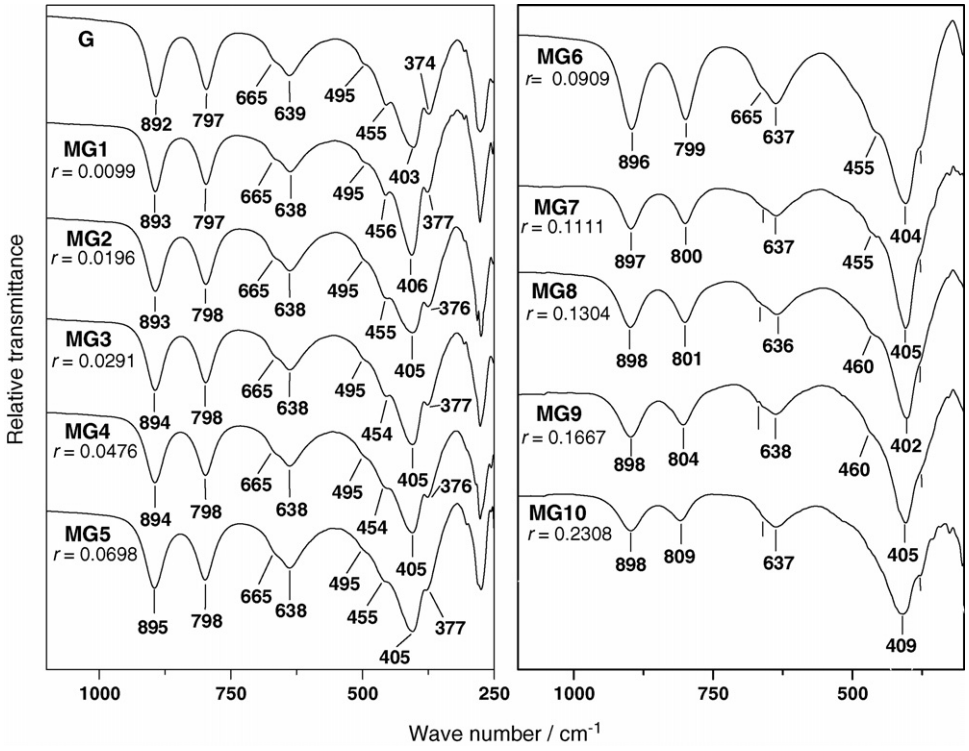

Fig. 5. FT-IR spectra of samples G, MG1–MG10 recorded at RT.

FT-IR spectra were recorded at RT using a Perkin-Elmer spectrometer, model 2000. The FT-IR spectrometer was linked to a personal computer with an installed IRDM (IR data manager) program to process the recorded spectra. The specimens were pressed into small discs using a spectroscopically pure KBr matrix.

A thermal field emission scanning electron microscope (JSM-7000F, manufactured by JEOL Ltd.) was used. FE SEM was linked to the EDS/INCA 350 (energy dispersive X-ray analyser) manufactured by Oxford Instruments Ltd.

3. Results and discussion

3.1. ^{57}Fe Mössbauer spectroscopy

Acicular and monodisperse α-FeOOH particles were precipitated in a highly alkaline medium (pH ∼ 13.5–13.8) using a strong organic alkali (TMAH) as the precipitating agent. This synthesis method showed high reproducibility that is very important in studying the formation of solid solutions inside an α-FeOOH structure. The main difference between NaOH (or KOH) on one side and TMAH on the other is that in the case of TMAH the initially formed precipitate ("amorphous" $Fe(OH)_3$ or the ferrihydrite-like phase) is completely dissolved at RT on strong shaking, as observed with the naked eye. Upon a short ageing time homogenous α-FeOOH recrystallisation was achieved [21].

Fig. 1 shows the RT Mössbauer spectrum of α-FeOOH (sample G) prepared by this synthesis route. It is visible that the spectral lines are broadened and that they deviate from the theoretical intensity ratios 3:2:1:1:2:3. The RT Mössbauer spectrum of α-FeOOH may vary from a well-shaped sextet up to one paramagnetic doublet, which depends on the size and crystallinity of α-FeOOH particles. For example, α-FeOOH particles smaller than ∼15–20 nm show a superparamagnetic type of the Mössbauer spectrum at RT. On the other hand, α-FeOOH particles smaller than 8 nm show a superparamagnetic type of the

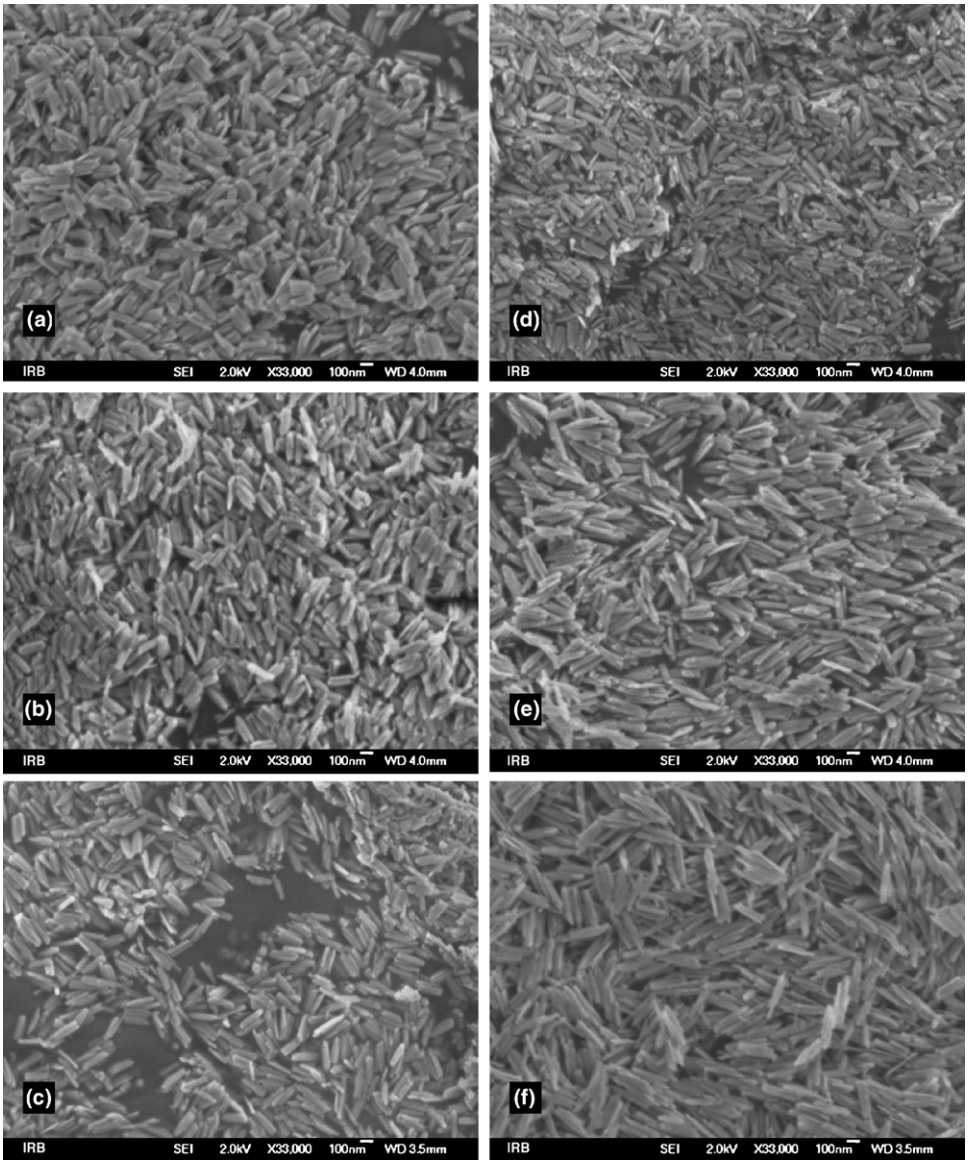

Fig. 6. FE SEM micrographs of samples (a) G, (b) MG1, (c) MG3 and (d–f) MG4–MG6.

Mössbauer spectrum down to 77 K [23]. Incorporation of metal cations into the α-FeOOH structure induces a broadening of diffraction lines and a decrease in the average hyperfine magnetic field. This effect is different for various metal cations, but it is also dependent on the synthesis route of α-FeOOH. For that reason it is important to achieve the reproducibility of the α-FeOOH synthesis.

Fig. 1 shows a progressive broadening of Mössbauer lines and increased intensity of inner lines with an increase in the concentration of Mn-dopant. The Mössbauer spectrum of sample MG9 ($r = 0.1667$) was fitted for an additional doublet Q. The sextet collapsed completely in the case of sample MG10 ($r = 0.2308$). Only a paramagnetic doublet was recorded instead. The parameters, $\delta = 0.37\ \mathrm{mm\ s^{-1}}$ and $\Delta = 0.55\ \mathrm{mm\ s^{-1}}$, calculated for the spectrum of sample MG10, were taken in the fitting procedure for sample MG9. Table 2 shows RT Mössbauer parameters calculated for samples G to MG10. Fig. 2 shows the distribution of HMF for α-FeOOH (sample G) and samples MG1–MG9 (samples α-(Fe, Mn)OOH). A progressive broadening of HMF distribution and a shift of the distribution maximum to lower B_{hf} values are well visible. The average B_{hf} value ($\langle B_{hf}\rangle = 34.9$ T) recorded for undoped α-FeOOH decreased to $\langle B_{hf}\rangle = 21.4$ T for Mn-doped α-FeOOH ($r = 0.1667$). A linear least squares regression analysis revealed a linear dependence of $\langle B_{hf}\rangle$ values versus $r = [Mn]/([Mn] + [Fe])$ up to $r = 0.1667$, as shown in Fig. 3. The presence of α-Fe_2O_3 was not observed, even at higher initial concentrations of manganese ($r > 0.2308$). However, Mössbauer measurements showed the formation of a ferrite phase at $r = 0.3333$, besides α-(Fe, Mn)OOH. Fig. 4 shows RT Mössbauer spectrum of sample MG11 ($r = 0.3333$). This spectrum was considered as superposition of a paramagnetic doublet and four sextets. The paramagnetic doublet can be assigned to α-FeOOH particles with maximal amount of Mn-dopant. The sextet M_1 with hyperfine field distribution and $\langle B_{hf}\rangle = 19.8$ T can be assigned to the fraction of α-(Fe, Mn)OOH particles with a smaller amount of Mn-dopant. This means that in sample MG11 there is a broad distribution of Mn-dopant concentration between α-(Fe, Mn)OOH particles. In the first attempt, ferrite phase in the sample MG11 was fitted for two sextets; however, a significantly better fit was obtained with three sextets, M_2, M_3 and M_4. These sextets can be assigned to ferrite phase with general composition $Mn_xFe_{3-x}O_4$. This fitting approach is consistent with that proposed by Persoons et al. [24]. These authors have investigated Co-substituted magnetites, $Co_xFe_{3-x}O_4$, for compositions $x = 0.6$, 0.8 and 0.9 and the corresponding Mössbauer spectra were fitted with a superposition of one A-site subspectrum and three B-site subspectra. According to these authors, A-site distribution remains sharp and quite symmetric, whereas the shape of the B-site hyperfine field distribution for the substitution $x = 0.6$, 0.8 and 0.9 is much more complicated and indicates the presence of several average charge states for the iron species.

Our results are in accordance with the works by Stiers and Schwertmann [15] and Cornell and Giovanoli [25] who have shown by chemical analysis that up to ∼15 mol% Mn could be incorporated into the α-FeOOH structure. Furthermore, our Mössbauer characterisations have shown that under a well-defined and reproducible synthesis of reference α-

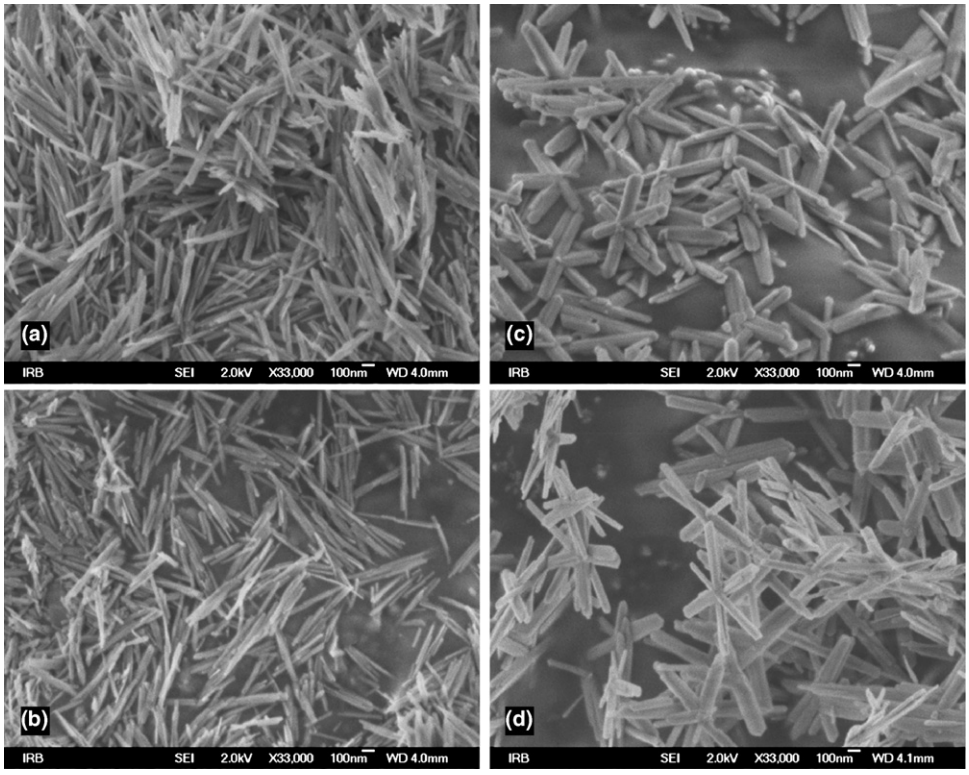

Fig. 7. FE SEM micrographs of (a and b) samples MG7 and MG8, and (c and d) sample MG10 (two details).

FeOOH, as well as Mn-doped α-FeOOH, the $\langle B_{hf} \rangle$ value can be used as a good indicator in the quantitative evaluation of Mn-doping.

3.2. FT-IR spectroscopy

Characteristic parts of the FT-IR spectra of samples G to MG10 are shown in Fig. 5. The spectrum of sample G shows all features of α-FeOOH conforming to reference literature data [26–29]. The effect of Mn-dopant on the FT-IR spectrum of α-FeOOH is visible. Fe–OH bending bands at 892 and 797 cm^{-1} (sample G), characteristic of α-FeOOH, are shifted to higher wave numbers. For example, the band at 892 cm^{-1} is shifted to 898 cm^{-1} (sample MG10), whereas the band at 797 cm^{-1} is shifted to 809 cm^{-1} (sample MG10). Stiers and Schwertmann [15] observed IR shifts at 888.1–893.3 and 791.7–800.6 cm^{-1} for Fe–OH bending vibrations in Mn-substituted α-FeOOH. The concentration range for x varied from $x = 0$ to 0.179 in α-$Fe_{1-x}Mn_xOOH$. However, these band positions (δ_{OH} and γ_{OH}) are far from those recorded for α-MnOOH (groutite; $\delta_{OH} = 1029\ cm^{-1}$; $\gamma_{OH} = 996\ cm^{-1}$). Recently, Alvarez et al. [30] have investigated by XRD the effect of Mn^{2+} incorporation on the transformation of ferrihydrite to α-FeOOH and considered a possible oxidation of Mn^{2+} to Mn^{3+}, as in the work by Stiers and Schwertmann [15]. Fig. 5 also shows that there is no significant shift of Fe–O stretching bands with an increase in r up to 0.2308. Careful inspection of the FT-IR spectra of samples MG1–MG10 showed very weak bands (these parts are not shown in Fig. 5) which can be assigned to specifically adsorbed sulphate groups. The intensity of these IR bands slightly increased with an increase in the initial $MnSO_4$ concentration. The assignation of sulphate groups in the present samples was based on data given by Musić et al. [31]. Generally, the adsorption of anions on metal (hydrous) oxide particles decreases to zero at high pH values. However, in the case of specifically adsorbed oxyanions, traces or small amounts can be detected in precipitates at high pH values [32]. FT-IR spectroscopy applied in the present work has shown this technique to be just a qualitative indicator of the changes in α-(Fe, Mn)OOH depending on r.

3.3. FE SEM

FE SEM observation showed distinct changes in the size and geometrical shape of Mn-substituted α-FeOOH particles. With an increased Mn-substitution there is a gradual increase in the length of α-FeOOH crystallites along the c-axis, as shown in Fig. 6. The maximum elongation, up to ~5 times, was shown for samples MG7 and MG8 (Fig. 7a and b). Elongation of α-(Fe, Mn)OOH particles could be enhanced by the preferential adsorption of manganese ions along the c-axis. The adsorption of metal cations increases with an increased pH [33], which is opposite to the adsorption behaviour of anions. It is also well known that adsorbed sulphate groups enhance the elongation of metal (hydrous)oxide particles.

With further increase in the Mn-substitution ($r = 0.1667$ for sample MG9; $r = 0.2308$ for sample MG10) the geometrical form of α-(Fe, Mn)OOH particles significantly changed, as shown in Fig. 7c and d. Star-shaped and dendritic α-(Fe, Mn)OOH particles were formed. Moreover, the widths of these particles increased, whereas their edges were much better shaped than in the case of α-(Fe, Mn)OOH particles shown in Fig. 7a and b. The morphologies of α-(Fe, Mn)OOH particles observed by FE SEM are in line with the TEM results by Cornell and Giovanoli [25]. Fig. 8a and b shows FE SEM micrographs of sample MG11 taken at different optical magnifications. These micrographs show big α-(Fe, Mn)OOH rods of different sizes (lengths, as well as widths). This is consequence of nonuniform distribution of Mn-dopant between α-(Fe, Mn)OOH particles for $r = 0.3333$, as already concluded in analysis of the Mössbauer spectrum of sample MG11. In the same micrographs, besides α-(Fe, Mn)OOH particles, much smaller particles (and their aggregates) are also visible, which can be assigned to ferrite phase ($Mn_xFe_{3-x}O_4$). This finding is similar to the results obtained by Sileo et al. [34]. These authors have found a mixture of jacobsite- and goethite-like phases in the same proportion for $r = 0.28$, whereas jacobsite as major phase and hausmanite as minor phase were found for $r = 0.55$.

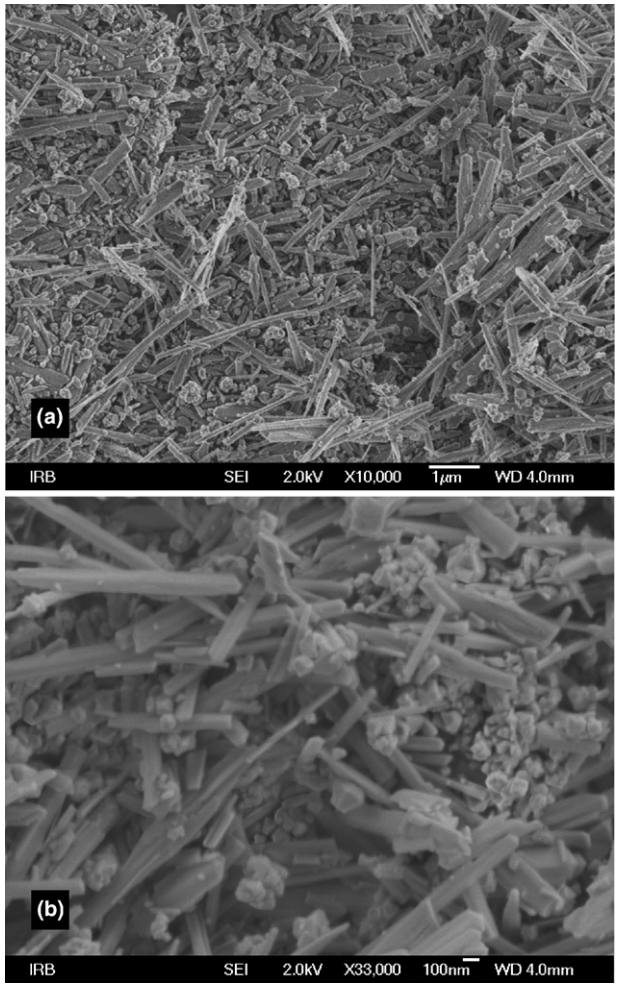

Fig. 8. FE SEM micrographs of sample MG11 at (a) lower optical magnification and (b) higher optical magnification.

4. Conclusion

- Acicular and monodisperse α-FeOOH particles were precipitated by adding the solution of a strong organic alkali to an $FeCl_3$ solution at pH ∼ 13.5–13.8 and autoclaving the precipitation system at 160 °C. Thus synthesised α-FeOOH was used as a reference material in the investigation of the influence of Mn-dopant on the formation of α-(Fe, Mn)OOH solid solutions and on the changes in the size and morphology of corresponding α-(Fe, Mn)OOH particles.
- RT Mössbauer spectra showed a progressive broadening of spectral lines and increased intensity of inner lines with an increase in the concentration of Mn-dopant in the α-(Fe, Mn)OOH structure. $\langle B_{hf} \rangle$ value of 34.9 T recorded for α-FeOOH decreased linearly down to 21.4 T for sample with $r = 0.1667$, where $r = [Mn]/([Mn] + [Fe])$. The sextet collapsed completely at RT for the ratio $r = 0.2308$; only a paramagnetic doublet was recorded instead. A ferrite phase was additionally found for $r = 0.3333$; however, the presence of an α-Fe_2O_3 phase was not observed in any of the prepared samples.
- FT-IR spectra of α-(Fe, Mn)OOH samples showed gradual shifts of Fe–OH bending bands, δ_{OH} and γ_{OH}, with an increased Mn-substitution. Also, FT-IR spectra showed the IR bands of very weak intensities which can be assigned to preferentially adsorbed sulphates on α-(Fe, Mn)OOH particles.
- FE SEM micrographs showed a maximum elongation up to ∼5 times of acicular α-FeOOH particles along the *c*-axis with Mn-doping at $r = 0.1111$ and 0.1304. At the concentration ratios $r = 0.1667$ and 0.2308 the star-shaped and dendritic twin particles were observed.

References

[1] F.J. Berry, Ö. Helgason, A. Bohórquez, J.F. Marco, J. McManus, E.A. Moore, S. Mørup, P.G. Wynn, J. Mater. Chem. 10 (2000) 1643–1648.
[2] D.G. Lewis, U. Schwertmann, Clay Miner. 14 (1979) 115–126.
[3] M.V. Fey, J.B. Dixon, Clays Clay Miner. 18 (1981) 91–100.
[4] E. Murad, U. Schwertmann, Clay Miner. 18 (1983) 301–312.
[5] D.G. Schulze, Clays Clay Miner. 32 (1984) 36–44.
[6] U. Schwertmann, U. Gasser, H. Sticher, Geochim. Cosmochim. Acta 53 (1989) 1293–1297.
[7] R. Balasubramanian, D.C. Cook, M. Yamashita, Hyp. Interact. 139–140 (2002) 167–173.
[8] H. Konishi, M. Yamashita, H. Uchida, J. Mizuki, Mater. Trans. 46 (2005) 337–341.
[9] S. Suzuki, Y. Takahashi, M. Saito, M. Kusakabe, T. Kamimura, H. Miyuki, Y. Waseda, Corros. Sci. 47 (2005) 1271–1284.
[10] C.A. Dos Santos, A.M.C. Horbe, C.M.O. Barcellos, J.B. Marimon da Cunha, Solid State Commun. 118 (2001) 449–452.
[11] E.E. Sileo, P.S. Solís, C.O. Paiva-Santos, Powder Diffr. 18 (2003) 50–55.
[12] M.L.M. de Carvalho-e-Silva, C.S.M. Partiti, J. Enzweiler, S. Petit, S.M. Netto, S.M.B. De Oliveira, Hyp. Interact. 142 (2002) 559–576.
[13] C. Sudakar, G.N. Subbanna, T.R.N. Kutty, J. Mater. Sci. 39 (2004) 4271–4286.
[14] S. Krehula, S. Musić, S. Popović, J. Alloys Compd. 403 (2005) 368–375.
[15] W. Stiers, U. Schwertmann, Geochim. Cosmochim. Acta 49 (1985) 1909–1911.
[16] R.E. Vandenberghe, A.E. Verbeeck, E. De Grave, W. Stiers, Hyp. Interact. 29 (1986) 1157–1160.
[17] R.M. Cornell, Clay Miner. 26 (1991) 427–430.
[18] B. Singh, D.M. Sherman, J.F.W. Mosselmans, R.J. Gilkes, M.A. Wells, Clay Miner. 37 (2002) 639–649.
[19] A.L. Morales, C.A. Barrero, F. Jaramillo, C. Arroyave, J.-M. Greneche, Hyp. Interact. 148–149 (2003) 135–144.
[20] T. Kusuyama, K. Tanimura, K. Sato, Mater. Trans. 43 (2002) 455–458.
[21] S. Krehula, S. Popović, S. Musić, Mater. Lett. 54 (2002) 108–113.
[22] F.J. Berry, Advances in Inorganic Chemistry and Radiochemistry, vol. 21, Academic Press, 1978, pp. 255–286.
[23] E. Murad, J.H. Johnston, in: G.J. Long (Ed.), Mössbauer Spectroscopy Applied to Inorganic Chemistry, vol. 2, Plenum Publishing Corporation, 1987, pp. 507–582.
[24] R.M. Persoons, E. De Grave, P.M.A. de Bakker, R.E. Vandenberghe, Phys. Rev. B 47 (1993) 5894–5905.
[25] R.M. Cornell, R. Giovanoli, Clays Clay Miner. 35 (1987) 11–20.
[26] C. Morterra, A. Chiorino, E. Borello, Mater. Chem. Phys. 10 (1984) 119–138.
[27] L. Verdonck, S. Hoste, F.F. Roelandt, G.P. Van der Kelen, J. Mol. Struct. 79 (1982) 273–279.
[28] P. Cambier, Clay Miner. 21 (1986) 191–200.
[29] B. Weckler, H.D. Lutz, Eur. J. Solid State Inorg. Chem. 35 (1998) 531–544.
[30] M. Alvarez, E.E. Sileo, E.H. Rueda, Chem. Geol. 216 (2005) 89–97.
[31] S. Musić, A. Šarić, S. Popović, K. Nomura, T. Sawada, Croat. Chem. Acta 73 (2000) 541–567.
[32] S. Musić, M. Ristić, M. Tonković, Z. Wasser, Abwasser-Forsch. 19 (1986) 186–196.
[33] S. Musić, M. Ristić, J. Radioanal. Nucl. Chem. 120 (1988) 289–304.
[34] E.E. Sileo, M. Alvarez, E.H. Rueda, Int. J. Inorg. Mater. 3 (2001) 271–279.